

---

# Facile Preparation of Smart Sponge Based on Zeolitic Imidazolate Framework for the Efficient Separation of Oily Wastewater

---

[Yu-Ping Zhang](#)<sup>\*</sup>, Xin-Xin Chen, Pei Yuan, Hai-E Chen, [Song-Wei Li](#)<sup>\*</sup>

Posted Date: 15 July 2024

doi: 10.20944/preprints202407.1118.v1

Keywords: Oil/water separation; Melamine sponge; ZIF-8; Smart material; Oil absorption



Preprints.org is a free multidiscipline platform providing preprint service that is dedicated to making early versions of research outputs permanently available and citable. Preprints posted at Preprints.org appear in Web of Science, Crossref, Google Scholar, Scilit, Europe PMC.

Copyright: This is an open access article distributed under the Creative Commons Attribution License which permits unrestricted use, distribution, and reproduction in any medium, provided the original work is properly cited.

Article

# Facile Preparation of Smart Sponge Based on Zeolitic Imidazolate Framework for the Efficient Separation of Oily Wastewater

Yu-Ping Zhang <sup>1,2,\*</sup>, Xin-Xin Chen <sup>2</sup>, Pei Yuan <sup>1</sup>, Hai-E Chen <sup>2</sup> and Song-Wei Li <sup>2,\*</sup>

<sup>1</sup> College of Chemistry and Materials Engineering, Hunan University of Arts and Science, Changde 415000, P. R. China. E-mail: beijing2008zyp@163.com

<sup>2</sup> Henan Institute of Science and Technology, Xinxiang 453003, P.R. China

\* Correspondence: beijing2008zyp@163.com (Y.Z.); lear9999@163.com (S.L.)

**Abstract:** Fabrication of durable materials with excellent oil adsorption capacity and separation performance for the treatment of oily wastewater is meaningful based on smart responsiveness. Herein, a solvent-responsive melamine sponge (MS) was developed via silanization followed by the in-situ growth of zeolitic imidazolate framework-8 (ZIF-8). Detailed characterization of the resultant composite MS was conducted using scanning electron microscopy (SEM), energy dispersive spectrometer (EDS), X-ray diffraction (XRD), and Fourier transform infrared spectroscopy (FTIR). The multiscale hierarchical MS substrate exhibited highly hydrophobic property in the pH range of 1-11, along with a satisfactory adsorption capacity in the range of 65.4-134.2 g/g for different oils. The modified surface transformed from superhydrophobicity/superlipophilicity to superhydrophilicity/underwater superoleophobicity upon ethanol wetting, reverting to its original superhydrophobic state upon drying. The separation flux of the MS substrate was above  $1.5 \times 10^4$  L/m<sup>2</sup>h for both oil and water removal, along with the separation efficiency more than 98.7%. No obvious changes of the separation performance after 50 successive immiscible oil/water separation indicated the excellent durability and robustness of the anchored ZIF-8 nanoparticles on the surface of modified MS substrate. More importantly, oil-in-water emulsion separation was successfully carried out via the ZIF-8 MS composite with a high separation efficiency over 99.1%. The developed smart sponge with high oil absorption capacity, excellent chemical stability and fire resistance exhibited a wide range of potential practical applications in the convenient treatment of oily wastewater.

**Keywords:** oil/water separation; melamine sponge; ZIF-8; smart material; oil absorption

## 1. Introduction

Oily water pollution and frequent oil spill event usually bring about a great impact on both human beings and the natural environment [1–3]. On the one hand, the unlawful issue of oily wastewater domestically and industrially has led to an apparent increase in water pollution; on the other hand, offshore oil spills have brought about large-scale marine oil pollution [4,5]. Rapid removal of oil and prevention of the spread of oil spills is thus essential and urgent to minimize its hazards to the local environment and ecology. In general, oil/water separation was usually involved several aspects such as immiscible light oil/water, immiscible heavy oil/water separation, oil-in-water (O/W) and water-in-oil (W/O) emulsion separation in the absence of surfactants, surfactant-stabilized emulsion separation and etc. So far, many novel oil/water separation strategies and advance materials have been attempted to address these issues [6–8].

Two typical separation methods are usually selected for the oil/water separation [9,10]. Using separation materials with superhydrophobic and superoleophilic properties, one is the “oil-removing” mode. Using separating media with opposing surface wettability (superhydrophilicity and superoleophobicity underwater) is another choice known as “water-removing.” Because of their inherent oleophilicity towards the former materials, oil can easily clog or foul them. Additionally, denser water than light oil typically forms a barrier layer above the separating medium, obstructing

the penetration of oil. As a result, these materials limit the practical application of separating immiscible oil/water mixtures or surfactant stabilized O/W emulsions. Water-removing materials, as opposed to the former materials, protect themselves from oil fouling due to their unique underwater properties of superhydrophilicity and superoleophobicity, which are more desirable for gravitational oil/water separation. Furthermore, they are better suited to specific applications such as high-viscosity oil separation, wastewater purification, and use as a fence for offshore crude oil leaks, among others.

As a fascinating organic-inorganic hybrid materials, metal-organic frameworks (MOFs) are increasingly developed as adsorbents or separation materials due to their highly tunable, large surface area and rich structure [11]. In the same way, MOFs with special superwetting and superantiwetting properties are generally selected as "water-removing" and "oil-removing" materials for the oily water treatment. Li and et al prepared a filter paper by in-situ layer-by-layer growth of Cu-MOFs combining with subsequent polydimethylsiloxane (PDMS) treatment. Highly efficient separation of immiscible oil-water mixtures and W/O emulsion was realized via the resultant paper with superhydrophobic and superoleophilic coating [12]. Dong group reported a novel copper mesh with underwater superoleophobic and underoil superhydrophobic property, and HKUST-1 MOFs with  $\text{Cu}_2(\text{OH})_2\text{CO}_3$  particles was used as the precursors during the preparation process. It was effectively applied for oil/water separation with a separation efficiency of 97% [13]. A stainless steel mesh with a micro-nano hierarchical structure was coated by UiO-66 nanocrystals via a facile solution immersion method. The mesh membrane with hydrophilicity and underwater superoleophobicity exhibited high separation efficiency and excellent water permeation flux for the mixture of oil and water [14].

In general, two-dimensional (2D) materials (membrane, mesh, and fabric) present some disadvantages such as their poor adsorption capacity, low separation efficiency and weak wettability stability in oily water treatment [15]. In contrast, 3D materials such as sponges, aerogels, and metallic foams, are believed to be superior advantages [16]. Azam et al [17] prepared a 3D separation material based on the porous polyurethane sponge, which was functionalized with ZIF-8 and stearic acid. High hydrophobicity (WCA=140.8°) and high oil-absorbing capacity (30.26 ~ 115.35 g/g) and good reusability were obtained for the oil/water separation. Tamsilian et al [18] developed a superhydrophobic nanocomposite polyurethane (PU) sponge with ZIF-8 and polydimethylsiloxane (PDMS) as the synergistical coatings and the highest oil absorption capacity of 58 g/g and excellent oil-water separation were obtained. Zhang et al [19] directly used an in situ growth method to encapsulate ZIF-67 on the melamine sponge (MS) materials and constructed efficiently an oil-water separation system. The successful self-assembly of ZIF-67 macroparticles on the surface of the 3D skeleton resulted in a highly hydrophobic modified MS with a WCA of more than 140°. Zhang and et al successfully encapsulated ZIF-8 on the MS substrate with the help of adhesive attraction of dopamine, and the as-prepared ZIF-8-PDA@MS displayed superhydrophobicity with a WCA of 162°, high adsorption capacities over 85.45 g/g and reusability over 40 times [17]. Recently, our group used a facile method of "double birds with one stone" to modify Ni foams via initial solvothermal synthesis of Fe/Ni MOF and subsequent solution immersion of stearic acid. Both processes led to the final foams with opposite surface wettability. The former Ni foam with the growth of superwetting MOF was superhydrophilic/underwater superoleophobic, which was suitable for the separation of light oil/water, the latter with further chemical modification was superhydrophobic/superlipophilic, which benefited for the collection of oil spill [21].

Motivated by the above studies, we prepared a smart composite by combining ZIF-8 with MS using a facile two-step strategy [18,22]. Prior to the in-situ ZIF-8 growth, the pristine MS had a smooth surface and lacked the activated growth sites. Therefore, the initial modification of the MS surface with (3-aminopropyl)triethoxysilane (APTES) was helpful to promote the coordination of free metal ions to its surface. The final APTES/ZIF-8/MS composites were systematically characterized by Scanning Electron Microscope (SEM), Energy Dispersive Spectroscopy (EDS), X-ray photoelectron spectroscopy (XPS) and Fourier Transform Infrared Spectroscopy (FTIR). With the characteristics of commercial MS and the highly hydrophobic ZIF-8, the as-prepared APTES/ZIF-8/MS composite

exhibited excellent oil adsorption capacity, efficient separation performance for immiscible oil/water and oil in water emulsion, as well as typical advantages such as antifouling, excellent recyclability, flame resistance and etc. More importantly, the smart composite sponge could undergo reversible change between superhydrophobicity/superoleophilicity and superhydrophilicity/underwater superoleophobicity, which was convenient for the switchable applications of both water-removal and oil-removal with the help of solvent responsiveness.

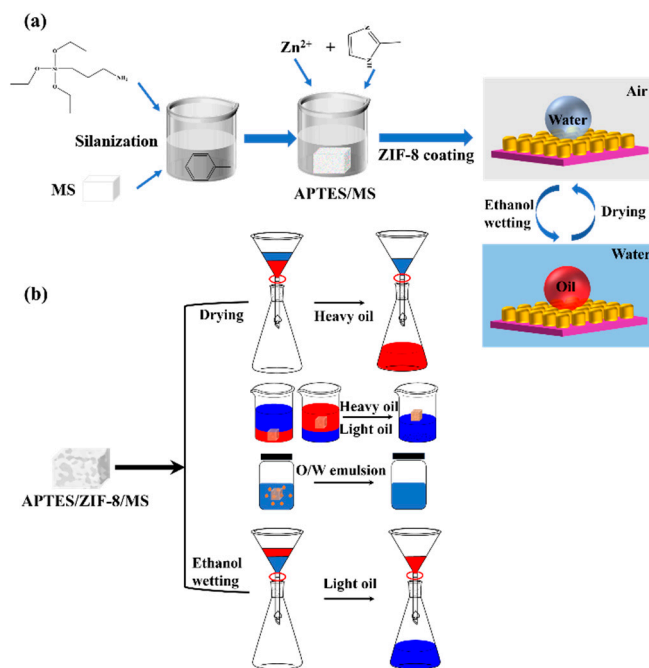
## 2. Experimental Section

### 2.1. Materials

Melamine sponge was purchased from the internet. Zinc nitrate hexahydrate (AR) was purchased from Tianjin Kemiou Chemical Reagent Co., Ltd. Methanol (HPLC grade), ethanol ( $\geq 99.8\%$ ), methylene blue trihydrate (indicator grade), Sudan III (AR), n-hexane, petroleum ether, iso-octane, n-octane, Span80, sodium hydroxide (96%) and hydrochloric acid (AR) were from Aladdin (Shanghai). N, N-dimethylformamide (DMF,  $\geq 99.9\%$ ). Toluene (AR) were purchased from Shanghai Energy Chemical Co. 2-Methylimidazole (98%) and (3-aminopropyl) triethoxysilane (APTES, 98%) were from Shanghai Titan Technology Co.

### 2.2. Preparation of ZIF-8/APTES/MS

First, the MS material was cut into  $2\text{ cm} \times 2\text{ cm} \times 2\text{ cm}$  pieces and washed by ultrasonication with deionized water and ethanol, respectively, for 10 min, and then dried in an oven at  $80^\circ\text{C}$ . The cleaned MS was immersed in 10 mL of toluene with the addition of  $30\ \mu\text{L}$  of APTES in a water bath at  $100^\circ\text{C}$  for 90 min. At room temperature, the cooled APTES/MS composite was rinsed with ethanol, so the unreacted compounds such as APTES, toluene and etc were then removed. Finally, the resulted APTES/MS was dried at  $80^\circ\text{C}$ . Both zinc nitrate hexahydrate (12.5 mmol) and 2-methylimidazole (25 mmol) dissolved in 50 mL of methanol, respectively, were quickly mixed and stirred thoroughly until fully dissolved. Then the as-prepared APTES/MS was then dipped into the mixed solution at room temperature for 6 h. Finally, the ZIF-8/APTES/MS composites were obtained by thorough washing with methanol and drying at  $80^\circ\text{C}$  for 12 h. The whole preparation process of this composite was illustrated in **Scheme 1a**, which included initial silanization of APTES, subsequent growth of Zif-8 and the switch of superwettability triggered by ethanol. Moreover, using the as-prepared APTES/ZIF-8/MS, multiple applications were shown in **Scheme 1b**, which was consisted of the oil removal, the efficient absorption to the floating light oil above the water surface and the heavy oil underwater, the separation of O/W emulsion using the drying MS, and the water removal using the MS wetted by ethanol, respectively.



**Scheme 1.** Preparation and application of ZIF-8/APTES/MS composites. (a) chemical modification and in-situ growth; and (b) multiple application for oily water.

### 2.3. Adsorption Experiments for Oil and Organic Solvent

Considering that oil and some organic reagents are common pollutants in water, we chose different oils (n-hexane, petroleum ether, toluene,  $\text{CCl}_4$ , and soybean oil) and organic solvents (methanol, ethanol, and DMF) for the investigation of the adsorption capacity of ZIF-8/APTES/MS composites. The oil-absorbing capacity of the sponges in different compositions and states was tested by immersing the sponges in various organic solvents and oils for 1 min at room temperature and weighing the mass of the sponges before and after oil absorption. All experiments were repeated at least three times. The oil absorption  $Q$  (g/g) was calculated according to Equation 1[23,24]:

$$Q = \frac{M_1 - M_0}{M_0} \quad (1)$$

where  $Q$  is the adsorption capacity of the composite for oil,  $M_0$  is the mass of the original ZIF-8/APTES/MS, and  $M_1$  is the mass of ZIF-8/APTES/MS after saturated adsorption by oil or organic solvent.

### 2.4. Recyclability and Reusability Tests

The as-prepared ZIF-8/APTES/MS materials were immersed into chloroform solution until saturated. Then they were manually squeezed to recover absorbed oil, weighed and reused for the next cycle. The test was conducted to examine the effect of the composite's adsorption capacity and residual capacity for 10 consecutive cycles.

### 2.5. Oil/water Separation

The separation of immiscible oil-water mixtures was carried out using a glass funnel. Sudan red and methylene were used to dye the oil and water phases, respectively. A small piece of ZIF-8/APTES/MS substrate was put at the funnel neck as an intermediate filtration layer. The separation flux ( $F$ ) and separation efficiency ( $\eta$ ) were calculated according to Equations 2 and 3 [24]:

$$F = V/A\Delta t \quad (2)$$

where  $V$  (L) stands for the volume of filtrate,  $A$  ( $m^2$ ) stands for the effective area of the filter layer, and  $\Delta t$  (h) stands for the separation time.

The separation efficiency is calculated as the ratio of the initial water mass ( $m_0$ ) to the separated water mass ( $m_1$ ) when no more droplets eluted from the glass funnel and is expressed in equation (3).

$$\eta = (m_1/m_0) \times 100\% \quad (3)$$

## 2.6. Emulsion Separation

To further investigate the adsorption capacity of ZIF-8/APTES/MS composites, surfactant-stabilized O/W emulsions were prepared. 1 mL of n-hexane was added to 99 mL of water with 0.1 g of surfactant (Span 80), and the homogenizer (5000 r/min) was stirred for 5 min to obtain surfactant-stabilized O/W emulsions.

The separation efficiency  $\eta$  (%) of the O/W emulsions was calculated according to the methods in the literature. Specifically, the absorbance of the emulsion and filtrate was determined by UV-Vis spectrophotometer and calculated using Equation 4 [24,25]:

$$\text{Separation efficiency} = \left(1 - \frac{I_1}{I_0}\right) \times 100\% \quad (4)$$

Where  $I_0$ ,  $I_1$  are the absorbance of the emulsion and filtrate, respectively.

## 2.7. Characterization

The microstructure and elements of the pristine sponges and ZIF-8/APTES/MS composites were investigated using a field emission SEM (Ultra Plus (Carl Zeiss)) and an EDS (Oxford X-MAX). The surface chemistry of the samples was analyzed by XPS (Thermo Scientific ESCALAB Xi+). FTIR (Japan-Shimadzu-IR Tracer 100) was used to determine the functional groups before and after modification for the MS composites. The absorbance of the emulsions and their filtrates was determined using a UV-Vis Spectrophotometer (Lambda 750 S), and the distribution of oil droplets in the filtrates and emulsions was observed by fluorescence microscopy (Nexcope NE620LED, USA). Surface wettability was assessed using an optical contact angle meter (TST-300H, Shenzhen, China). The contact angles (CAs) of oil and water droplets (6  $\mu$ L) were measured in the air and underwater conditions at room temperature. The static CA was calculated based on the average values from more than three different locations on the same substrate.

## 3. Results and Discussion

### 3.1. Characterization of ZIF-8/APTES/MS Composites

#### 3.1.1. SEM Analysis

To investigate the morphology of ZIF-8 crystals on sponges, the microstructures of pristine sponges, ZIF-8/MS and ZIF-8/APTES/MS were comparatively characterized by SEM. The pristine sponge had a micron-sized (50-100  $\mu$ m) porous cross-linked structure (**Figure 1a**) and a relatively clean and smooth backbone (**Figure 1b**). If APTES was not used to modify the sponge before ZIF-8 crystallization, the network structure and porosity of the obtained ZIF-8/MS were similar to that of the pristine sponges, and ZIF-8 crystalline particles were hardly observed (**Figure 1c and 1d**), which demonstrated that chemical modification is indispensable for the successful growth of ZIF-8 nanoparticles. Therefore, APTES molecules as the bridges on the sponge surface provided more  $NH_2$  groups and low surface energy chains for the immobilization of ZIF-8 nanoparticles in order to improve the hydrophobicity [26]. In addition, the 3-aminopropylsilyl group of APTES cooperated with the free  $Zn^{2+}$  center to directly bind the grown nanocrystals, so the surface of the ZIF-8/APTES/MS surface skeleton became very rough, and the magnified view (**Figure 1f** and its inset)

clearly showed that the sponge surface formed a dense yet rough ZIF-8 crystal layer, which was the key to construct a hydrophobic surface [27,28].

In order to calculate the distribution of the elements, the corresponding elemental compositions and energy spectra were further plotted. From **Figure 2a and 2b**, it demonstrated that the pristine sponge contained the elements C, N and O with the contents of 37.64%, 50.59% and 11.77%, respectively. However, in addition to the above three elements, elements Si and Zn were also present in the ZIF-8/APTES/MF composites with contents of 1.45% and 3.11%, respectively. The increase of the Si content resulted from the presence of the APTES molecules, while the significant increase in the Zn element suggested that the ZIF-8 nanoparticles were successfully adhered to the MS substrate. The EDS pattern of ZIF-8/APTES/MF clearly displayed the uniform distribution of elements C, N, O, Si and Zn on the sponge skeleton (**Figure 2c**).

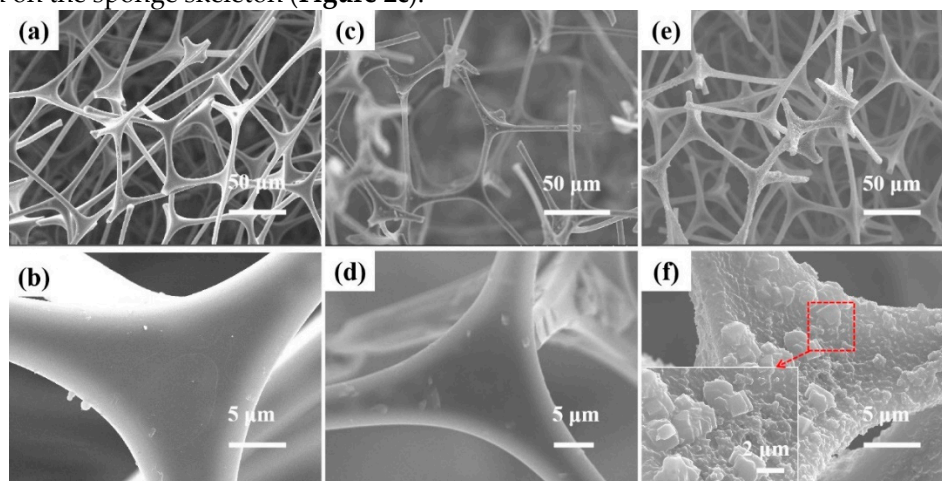


**Figure 1.** SEM of (a, b) pristine sponge, (c, d) ZIF-8/MS and (e, f) APTES/ZIF-8/MS composite.

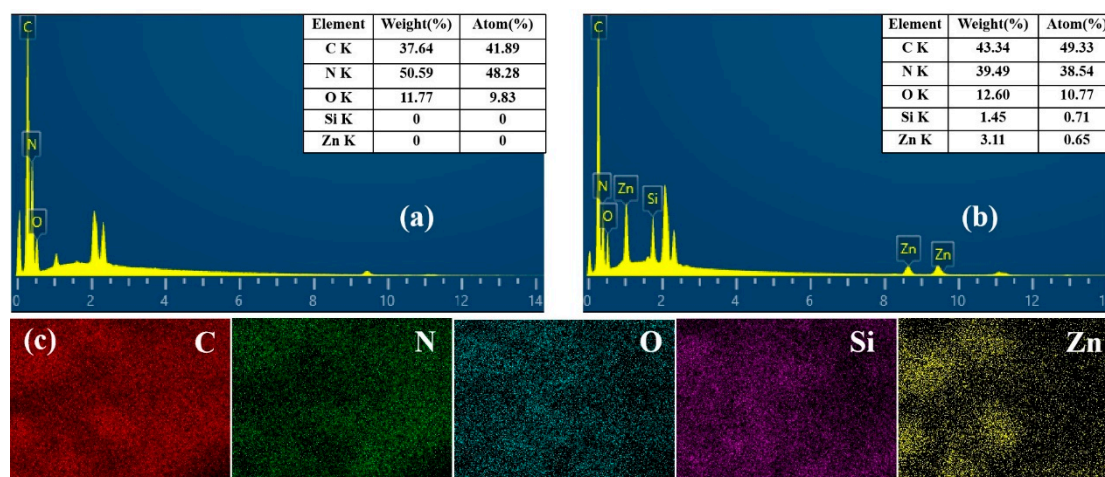


**Figure 2.** (a) EDS image of pristine sponge, (b and c) EDS image and elemental distribution of ZIF-8/APTES/MS composite, respectively.

### 3.1.2. XPS Analysis

XPS was used to analyze the changes in the chemical composition of the sponge surface before and after modification. As shown in **Figure 3a**, the primitive sponge contained mainly C, N and O elements. The XPS gross spectrum of the modified sponge exhibited an increase in the peak intensities of C 1s and O 1s, and a slight decrease in the peak intensity of N 1s, which could be attributed to the incorporation of APTES. Notes that it is rich in elemental C and O on the surface of APTES. More importantly, two new peaks were found at 102.02 eV and 1022.11 eV for elemental Si and Zn, which further proved the successful modification of APTES and the successful growth of ZIF-8 nanoparticles. The above results were consistent with the EDS patterns. In addition, the fitting of Zn

2p and Si 2p peaks were analyzed separately. In **Figure 3b**, asymmetric peak shapes were observed at 101.86 eV for overlapping Si 2p<sub>3/2</sub> and Si 2p<sub>1/2</sub>, favorably demonstrating the successful modification of the MS by APTES molecules; and in **Figure 3c**, the Zn 2p<sub>3/2</sub> and 2p<sub>1/2</sub> occurred at 1022.08 eV and 1045.14 eV, demonstrating the presence of Zn<sup>2+</sup>.

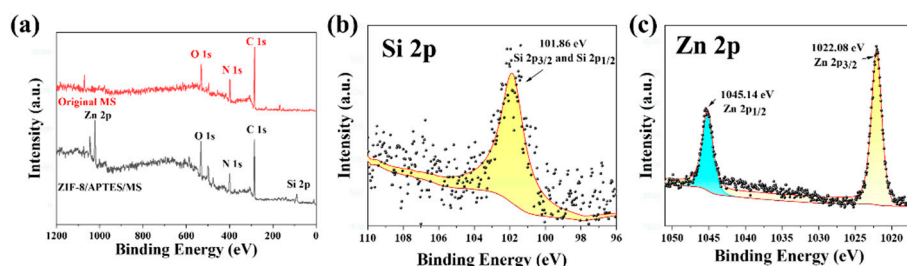


**Figure 3.** (a) XPS full spectra of pristine sponge and ZIF-8/APTES/MF composite, where (b) high-resolution Si 2p, (c) high-resolution Zn 2p for the ZIF-8/APTES/MS composite.

### 3.1.3. FT-IR Analysis

In order to elucidate the structure and interaction between ZIF-8 and APTES/MF, the chemical structure changes on the membrane surface were measured by FTIR in **Figure 4**. New coordination bonds were formed without damaging the melamine skeleton in the pristine MS, and the composites showed slight peak shifts compared with the pristine sponges at 3320 cm<sup>-1</sup>, 1475 cm<sup>-1</sup>, 1326 cm<sup>-1</sup>, 1150 cm<sup>-1</sup>, 973 cm<sup>-1</sup>, 811 cm<sup>-1</sup>, and 744 cm<sup>-1</sup>, which indicated that the sponge structure remained intact after ZIF-8 coating. Most importantly, the characteristic band of ZIF-8/APTES/MS at 432 cm<sup>-1</sup> was highly related to the Zn-N stretching vibration, which further confirmed the existence of ZIF-8 crystals [18,20].

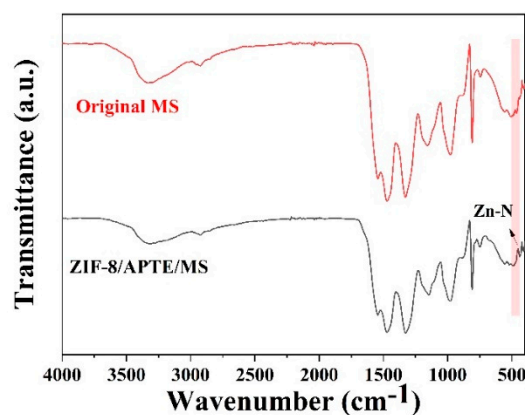


**Figure 4.** FTIR spectra of the original sponge and ZIF-8/APTES/MS.

### 3.2. Surface Wettability Analysis and Antifouling Properties

As shown in **Figure 5a and 5b**, a drop of water droplet (blue dyed by methylene blue) and a drop of oil (CCl<sub>4</sub>) droplet (red dyed with Sudan III) were dropped on the surface of the pristine sponge, respectively, and the water and oil droplets were immediately adsorbed, and the inset exhibited a WCA of 0°, indicating that the pristine sponge is amphiphilic [19]. In contrast, the water droplets on the surface of the ZIF-8/APTES/MS were spherical, with a WCA of up to 158.1°, while the oil droplets were adsorbed, suggesting that it was remarkable superhydrophobic/superoleophilic. When the pristine sponge and ZIF-8/APTES/MS were put into water, a significant difference was observed. The pristine sponge quickly sank to the water bottom due to its superhydrophilicity, whereas ZIF-8/APTES/MS floated on the water surface because of its superhydrophobicity (**Figure 5c**). However, when ZIF-8/APTES/MS was pressed below the surface of the water under an external

force, a shiny, reflective interface appeared, like a silver mirror. It was attributed that the special structure of the ZIF-8/APTES/MS surface formed an air layer on the surface and the trapped air bubbles around the surface created a “silver mirror” phenomenon on the underwater surface (**Figure 5d**). Interestingly, when the MS composite wetted by methanol contacted with oil, underwater superoleophobicity was observed with a UWOCA of  $154.2^\circ$  (**Figure 5e**) [29]. Even after a period of time, the oil droplet remained spherical on the ZIF-8/APTES/MS surface (**Figure 5f**). It should be noted that it regained its original superhydrophobicity after being dried. In addition, the identical wetting effects on ZIF-8/APTES/MS material were obtained using other solvents such as methanol, acetonitrile and DMF with each UWOCA over  $150^\circ$ . The polarity, surface tension and UWOCA for each solvent to trigger the responsiveness were listed in **Table 1**.

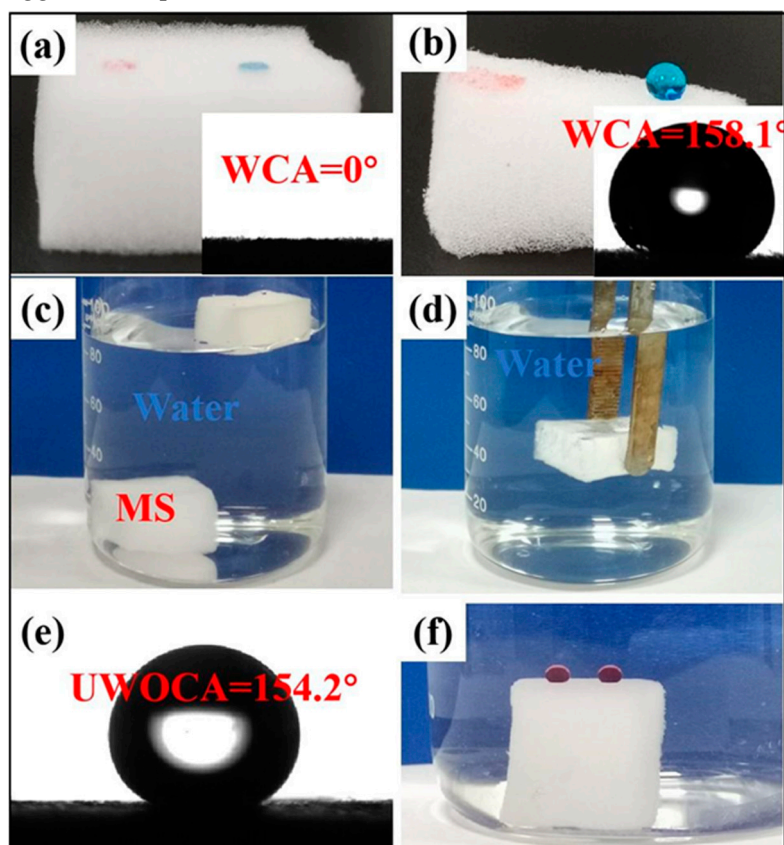


**Figure 5.** Photographs of  $\text{CCl}_4$  and water on the surface of (a) pristine sponge and (b) ZIF-8/APTES/MS composite (inset corresponds to the WCA), respectively; (c) photographs of ZIF-8/APTES/MS composite floating on the water surface and the pristine sponge sunk on the bottom of the water; (d) Photographs of ZIF-8/APTES /MS composites strongly immersed in water; (e) UWOCA of ZIF-8/APTES/MS composites after being wetted with ethanol, and (f) images of underwater superoleophobic oil droplets.

**Table 1.** The UWOCA values of ZIF-8/APTES/MS composites wetted by different organic solvents.

Solvent	Polarity	Surface tension (mN/m)	UWOCA ( $^\circ$ )
Methanol	6.6	23.6	151.7 $^\circ$
Ethanol	4.3	22.39	154.2 $^\circ$
Acetonitrile	6.2	22.75	153.1 $^\circ$
DMF	7.87	25.7	150.6 $^\circ$

The mechanism of the switchable superwettability from superhydrophobic/superoleophilic to superhydrophilic/superoleophobic underwater is explained as follows [30]: When a drop of water seats on the fabricated superhydrophobic surface, the trapped air in the micro/nano structures of the surfaces can keep the water droplet spherical in the air at the Cassie state (**Figure 6a**). At the same

time, the air layer on the superhydrophobic surfaces underwater reduces the water penetration. Whilst if one oil droplet contacts the surface underwater, it will infiltrate the air layer. As the MS composite is wetted by ethanol or other low surface energy liquid in **Table 1**, the voids in the micro/nano structures would be filled with ethanol instead of trapped air. Since ethanol molecules are highly solvable in water, they will be quickly diffused into the water layer and displaced by water molecules when the MS composites are immersed into water. As a result, the micro/nano structures on the wetted surface will be filled by water and formed Wenzel state (**Figure 6b**). Then the MS composite will exhibit superhydrophilicity/superoleophobic underwater before the MS material is dried again.

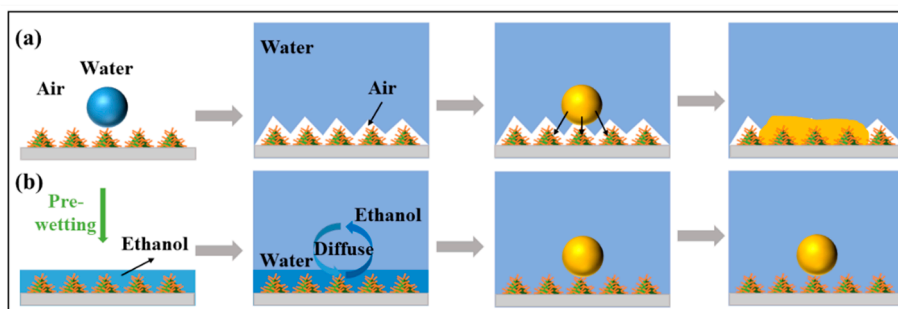


**Figure 6.** Mechanism of switchable wettability between superhydrophobic/underwater superoleophilicity and superhydrophilic/underwater superoleophobicity.

We systematically used a dynamic compression-separation process to further demonstrate the resistance of the prepared composite sponges to water or oil adhesion under different conditions. As shown in **Figure 7a**, a drop of water was used to slowly apply pressure to the dry state ZIF-8/APTES/MS composite in air. Although a large portion of the water droplet contacted with the surface of the composite, it did not detach from the tip, indicating that the resultant surface had significant resistance to water adhesion. Similarly, a drop of oil was slowly pressed onto the ethanol-wetted ZIF-8/APTES/MS composite in water. Although the oil droplet touched the surface of the sponge composite over a large area, it was lifted up without any trace (**Figure 7b**), and did not detach from the needle in the water, which indicated its excellent resistance to oil adhesion.

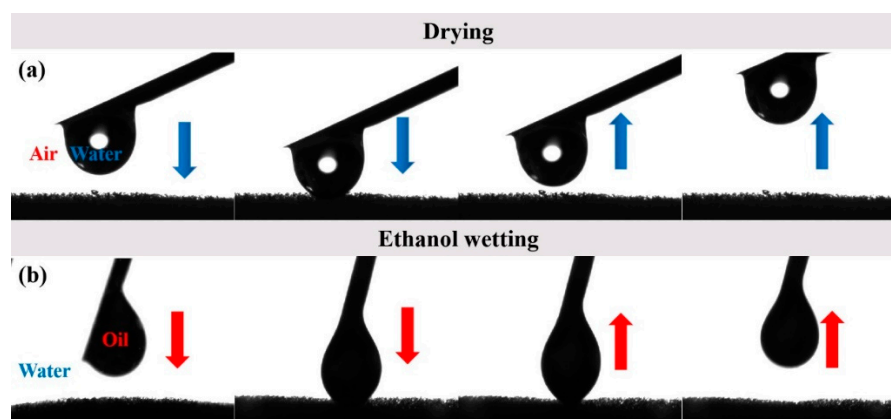


**Figure 7.** High-speed dynamic images. (a) water adhesion test in the air using the dried ZIF-8/APTES/MS composite; (b) oil adhesion test underwater using the wetted ZIF-8/APTES/MS composite.

### 3.3. Adsorption of Oil and Organic Solvents and Oil/Water Separation Properties

Due to its superhydrophobicity and high porosity, oil and organic reagents in water can be selectively adsorbed and collected via the ZIF-8/APTES/MS composite. Herein, the composites were comparatively used to separate light oil (n-hexane) and heavy oil ( $\text{CCl}_4$ ) from water. As shown in **Figure 8a** and **Figure 8b**, when the ZIF-8/APTES/MS composites were in contact with n-hexane or

$\text{CCl}_4$ , the oil was completely absorbed by the composites within a few seconds, and especially when the heavy oil was absorbed, the formation of a layer of bubbles at the solid-liquid interface could be clearly seen, which implied that spatial exchanges between the  $\text{CCl}_4$  and the air in the sponge structure took place, preventing the water from infiltrating into the sponge. It should be noted that both mixtures of light/heavy oil and water were completely adsorbed by the ZIF-8/APTES/MS, and there were no residual n-hexane and  $\text{CCl}_4$  droplets in the beaker after the adsorbed sponge was removed. In addition, the absorbed oil or organic solvent can be discharged by simple extrusion, thus enabling the reuse of ZIF-8/APTES/MS.

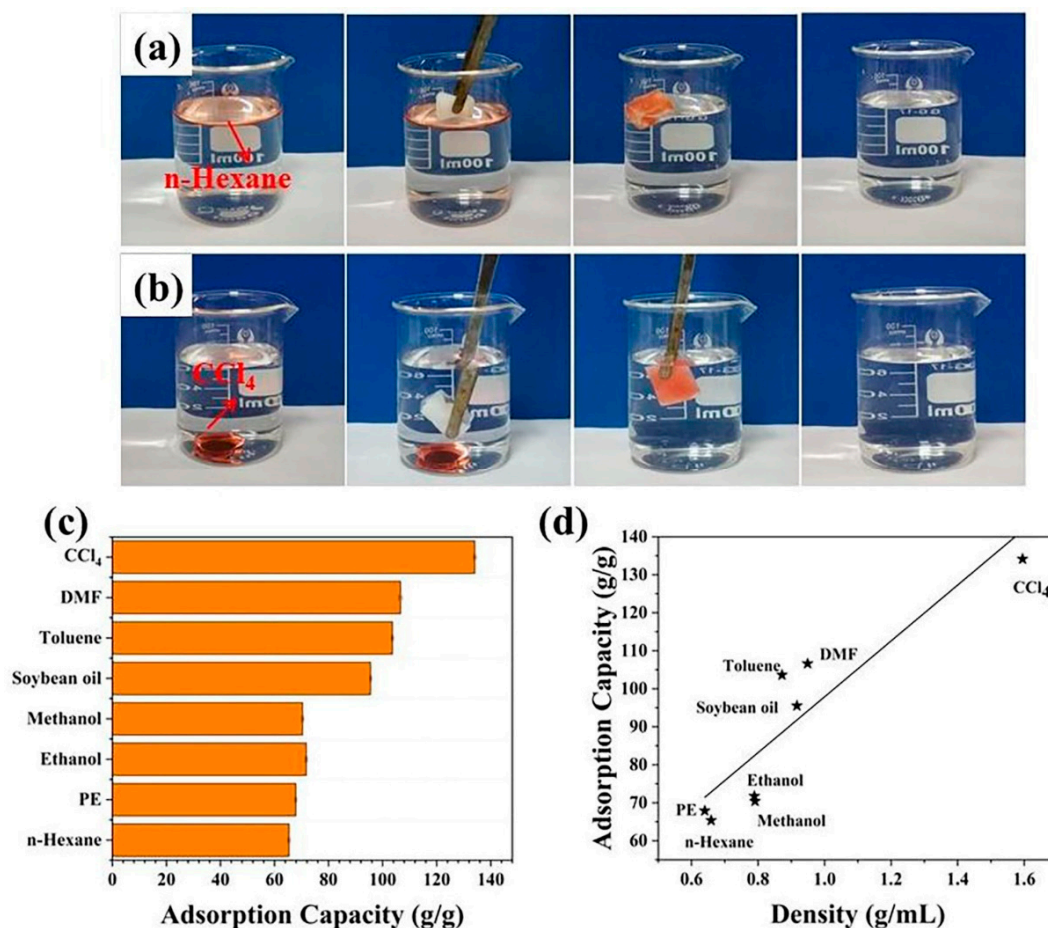


**Figure 8.** Photographs of the separation of (a) the mixture of n-hexane/water, (b) the mixture of  $\text{CCl}_4$ /water; (c) adsorption capacity of ZIF-8/APTES/MS composites; and (d) density of the organic solvents and oils versus adsorption capacity.

Organic reagents and oils discharged from laboratories and daily life, usually lead to some water pollution. Therefore, the adsorption capacity of ZIF-8/APTES/MS composite on different typical solvents and oils was further investigated including soybean oil, petroleum ether (PE), N,N-Dimethylformamide (DMF) and etc. The results showed that it exhibited a good adsorption capacity for eight kinds of oils and organic reagents, even up to 65.4 times (for n-hexane) to 134.2 times (for  $\text{CCl}_4$ ) of its own weight (see **Figure 8c**). In addition, the absorption capacities of previously reported ZIF-based/sponge composites were compared, and ZIF-8/APTES/MS had comparable or higher hydrophobicity and adsorption capacities, as listed in **Table 2**. Based on the fact that the adsorption capacity of sponges was highly related to the density of the absorbed reagent (**Figure 8d**) [31], and the higher density for the solvent or oil, the more adsorption capacity for the composite sponge.

**Table 2.** Comparison of adsorption properties of ZIF-8/APTES/MS composites with different ZIF-based/sponge composites.

Absorbents	WCA(°)	Absorption capacity(g/g)	Ref.
ZIF-8/SA/PU	143.2°	30.28-115.35	[32]
ZIF-8/PU	129.2°	28-79	[33]
ZIF-8/PE	-	17.6-55.8	[34]
ZIF-90/MS	154°	24-63	[36]
ZIF-8/PDMS/PU	156°	42-58	[18]
ZIF-8/APTES/MS	158.1°	65.4-134.2	This work

In addition, the reusability in practical applications for the ZIF-8/APTES/MS composites were investigated. Based on its superhydrophobicity and good absorbance of ZIF-8/APTES/MS,  $\text{CCl}_4$  was chosen as the experimental solvent and the absorption capacity and residual capacity were calculated for each cycle (see **Figure 9**). No significant decrease in absorption capacity and no obvious increase in residual capacity were found after 10 cyclic experiments. It was probably attributed to the good coverage and adhesion of the coating materials. The slight decrease in adsorption capacity was probably attributed to the following reasons [31,33]: insufficient squeezing of the residual adsorbed oil, structural damage of the sponge skeleton during the absorption-squeezing cycle, as well as the shedding of a small amount of ZIF-8 particles from the sponge.

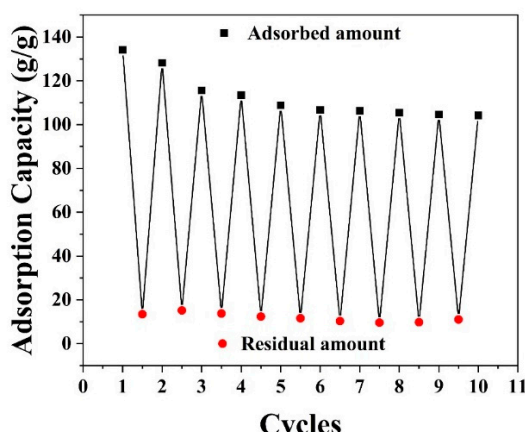


**Figure 9.** Reusability test of ZIF-8/APTES/MS composite for the adsorption of  $\text{CCl}_4$ .

The prepared ZIF-8/APTES/MS was immobilized in a funnel as shown in **Figure 10a** (marked with a red circle). Under normal drying conditions, ZIF-8/APTES/MS was superhydrophobic, so it was clearly observed that the red-dyed  $\text{CCl}_4$  rapidly penetrated the sponge and flowed into the beaker by its own gravity. Water was utterly blocked due to the superhydrophobic ZIF-8/APTES/MS and seated in the upper funnel. On the contrary, the sponge after being wetted by ethanol was superhydrophilic/superoleophobic underwater (see **Figure 10b**), the blue-dyed water rapidly passed the sponge gravitationally and n-hexane was thus blocked. The ZIF-8/APTES/MS composite was still solvent responsive after five ethanol wetting and drying cycles (**Figure 10c**), which was conveniently used for both separation modes of water and oil removal. Separation efficiencies and fluxes of various types of oil/water mixtures ( $\text{CCl}_4$ , n-hexane, n-octane, iso-octane, and petroleum ether) were comparably exhibited in **Figure 10d**. Regardless of whether water or oil was passed through the composite, excellent separation flux in the range of  $1.5 \times 10^4$  L/m<sup>2</sup>h to  $1.8 \times 10^4$  L/m<sup>2</sup>h were thus obtained, along with a high separation efficiency more than 98.7%. More meaningfully, only slight decrease of separation fluxes and stable separation efficiencies were found even after 50 consecutive cycles taking immiscible  $\text{CCl}_4$ /water and n-hexane/water mixtures as examples (**Figure 10e**). These results indicated that ZIF-8/APTES/MS composite was durable and robust for the treatment of oily water.

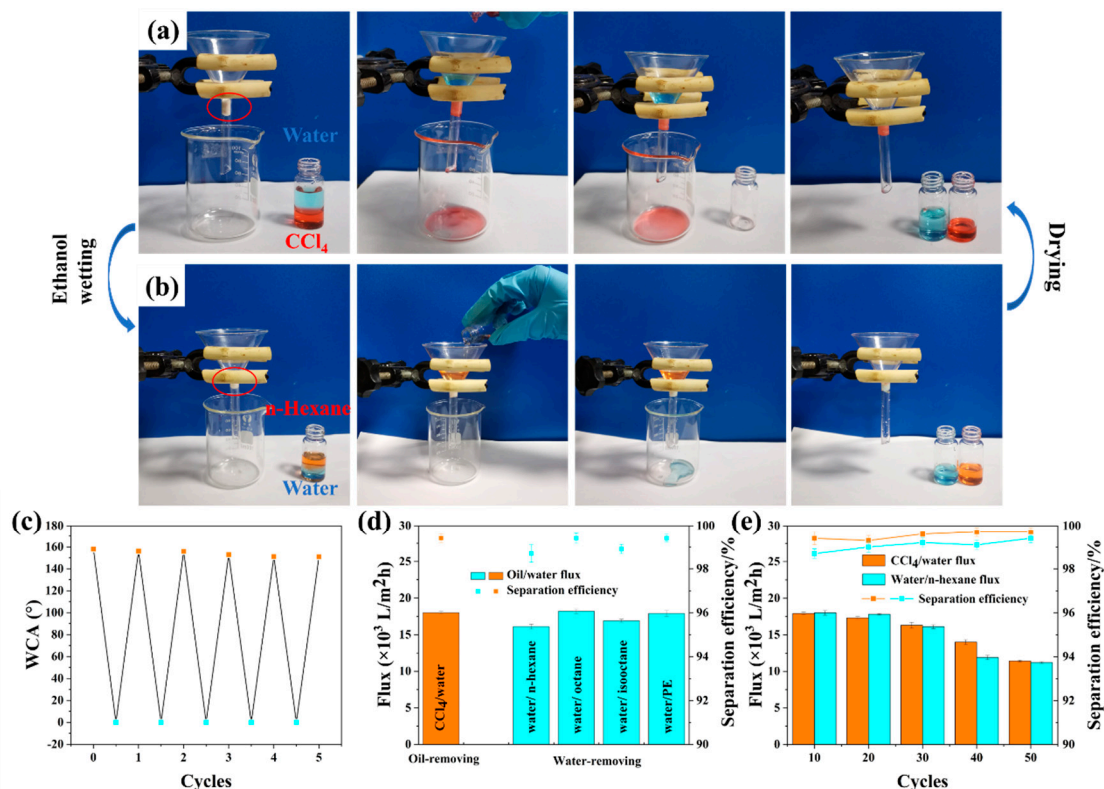


**Figure 10.** (a) Photographs of water/heavy oil separation under gravity-driven only (oil dyed with Sudan III and water dyed with methylene blue); (b) Photographs of light oil/water separation under gravity-driven only after ethanol wetting; (c) The changeable WCA for cyclic use for the ZIF-8/APTES/MS composites; (d) Separation efficiencies and fluxes for different oil/water mixtures; (e) The changes of separation efficiencies and fluxes during 50 cyclic oil/water separation for the immiscible CCl<sub>4</sub>/water and n-hexane/water mixtures.

### 3.4. Emulsion Separation

The treatment of emulsified oil/water mixture is more challenging and meaningful in practical application. Herein, we placed the composites in the oil (n-hexane)-in-water emulsion and moved them up and down rapidly for continuous absorption and compression, and the emulsion was clarified after a few minutes in **Figure 11a**. Additionally, it was apparently milky white for the emulsion before separation in **Figure 11b (inlet)**, and a great deal of oil droplets were obviously found with the help of the optical microscope. Comparatively, the emulsion after separation was transparent and colorless in **Figure 11c (inlet)**, and almost no oil droplets were detected. The separation efficiency was determined as high as 99.1%. It was more likely for the superhydrophobic composite to adsorb oil rather than water when it contacted the emulsion, and the water-repelling ability would be further improved if oil wetted the composite. The encapsulated ZIF-8 nanoparticles resulted in rougher surface with a stronger capillary force and a bigger surface area, which was beneficial for the adsorption of oil droplets and enabled the separation of oil-in-water emulsions.

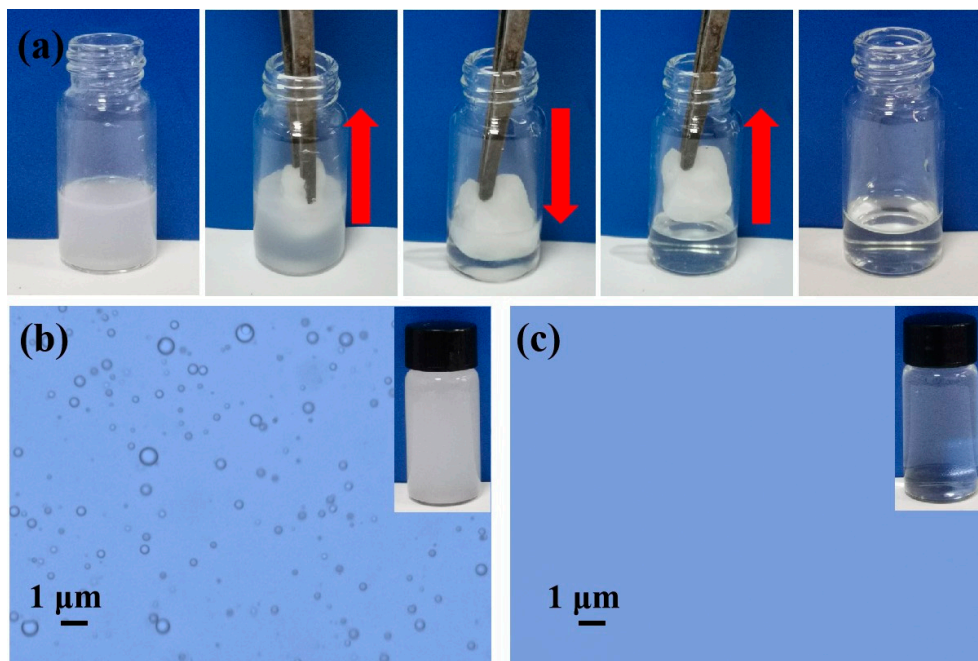


**Figure 11.** a. Process photographs for the oil (n-hexane)-in-water emulsion separation and (b, c) digital photographs and optical microscope images before and after separation.

### 3.5. Durability and Chemical Stability

Chemical stability of the as-prepared ZIF-8/APTES/MS composite is desirable for a long-term oily water treatment. The initial WCA was 158.1° for the superhydrophobic composite (see **Figure 12a**), and stable spheroid were maintained for a long time (120 min). However, in practice, the oil-containing wastewater may be acidic and alkaline. Therefore, it is needed to investigate the stability of its surface wettability under different pH conditions. As shown in **Figure 12b**, the results showed that the WCAs were 136.4° and 148.7°, under the extreme conditions of pH = 1 and pH = 11, respectively. It indicated that the as-prepared composite still exhibited high hydrophobicity under extreme conditions. It should be noted that the composite was superhydrophobic at near neutral pH conditions (the WCA is more than 150° at pH = 7).

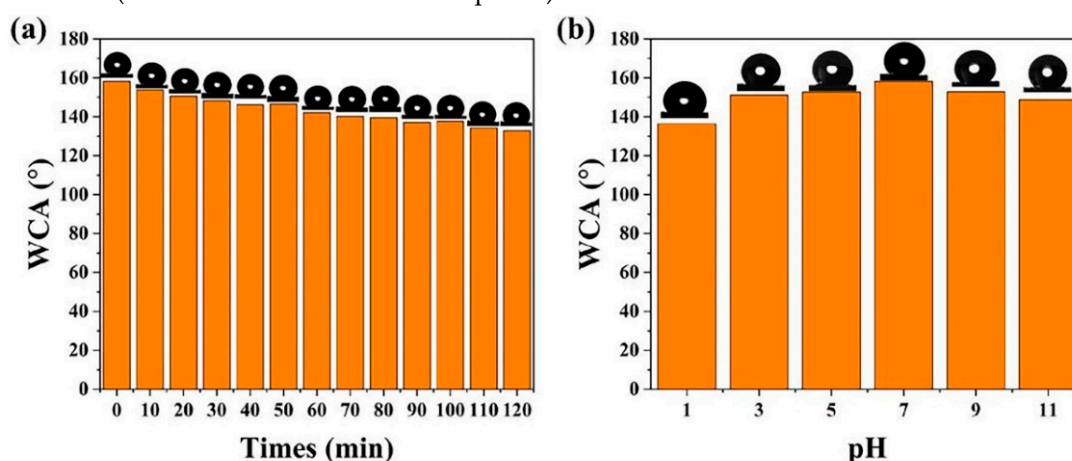


**Figure 12.** (a) WCA of ZIF-8/APTES/MS composites at different times; (b) WCA at different pH.

### 3.6. Flame Retardant

The fabricated ZIF-8/APTES/MS composite possessed excellent flame retardancy. Vigorous combustion did not occur for the pristine sponge when it contacted with an ignition source, and the

ignited sponge extinguished instantly without a heat source in **Figure 13a**. It was probably attributed that partial conversion from N element in the pristine sponge to  $N_2$ , NO and  $NO_2$  took place during the combustion process and the produced gases inhibited the material from continuous burn<sup>[32,33]</sup>. For the ZIF-8/APTES/MS composite, it demonstrated more excellent flame-retardant properties in the combustion test illustrated in **Figure 13b**. The composites inherited the natural flame retardancy of the pristine sponge, on the one hand, the attachment of APTES containing N element increased the whole N content in the final as-prepared sponge, and more gases of  $N_2$ , NO and  $NO_2$  were produced during the combustion, which was helpful for the prevention of further combustion; on the other hand, the zinc from the formed MOF also consumed the oxygen during the combustion process, which was also advantageous to its flame retardancy. Therefore, compared with the morphology of the pristine sponge, ZIF-8/APTES/MS still remained its original shape after combustion with less volume loss.

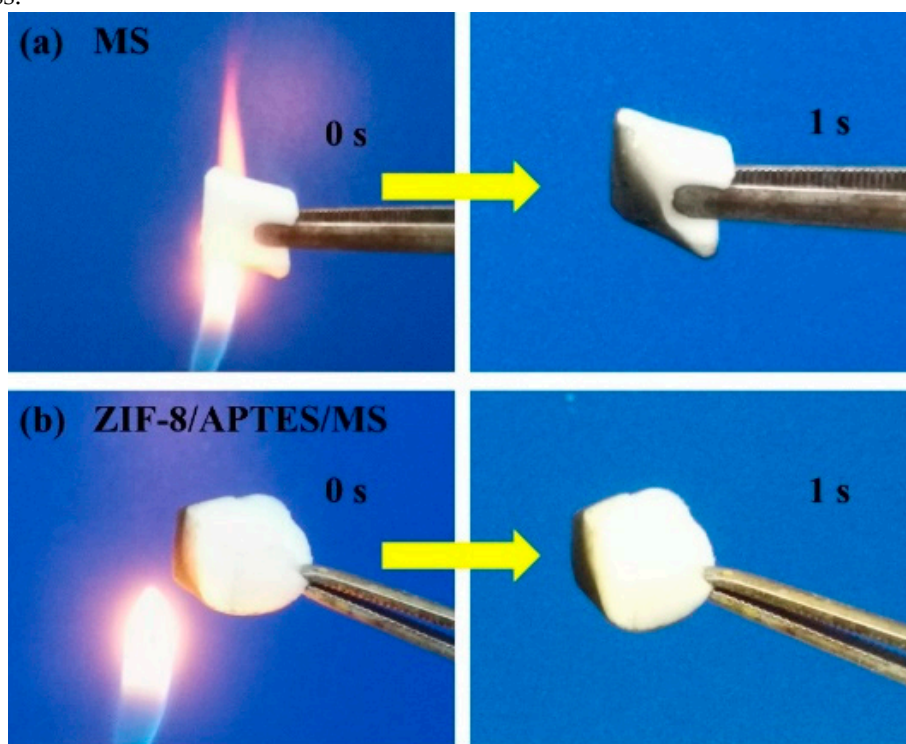


**Figure 13.** Combustion tests of (a) pristine sponge and (b) ZIF-8/APTES/MS composite.

#### 4. Conclusion

In summary, a type of novel coating material was developed with a switchable superwettability taking a commercial MS as a basic substrate. Two-step approaches were carried out by chemical modification of APTES and in-situ growth of ZIF-8. In combination of the exceptional porous and superhydrophobic capability of the ZIF-8 coatings and the ordered MS backbones, the final composite exhibited a high adsorption capacity of 65.4-134.2 g/g for various oils, high-flux oil/water separation efficiency and facile oil-in-water emulsion separation. Drying treatment and ethanol immersion yielded a rapid smart response between superhydrophobicity and underwater superoleophobicity. The resulted WCA was as high as  $158.1^\circ$  and the UWOCA was obtained more than  $154.2^\circ$ . Impressively, due to its compressibility and chemical stability, the fabricated MS sponge could be reused over 50 cyclic oil/water separations without significant change of the separation performance and easily recovered through simple squeezing. This novel composite is expected as a promising candidate for oil spill cleaning and conventional oily wastewater treatment.

**Declaration of Competing Interest:** The authors declare no conflict of interest.

**Acknowledgments:** This work was supported by the National Nature Science Foundation of China (22074029); the Start-up Project for High-Level Talents in HUAS and Hunan Provincial Key

Laboratory of Water Treatment Functional Materials; Key R&D and Promotion Special Project of Henan Province (212102110149).

## References

1. Wang Z, Guan M, Yang X, Li H, Zhao Y, Chen Y. A Trifecta membrane modified by multifunctional superhydrophilic coating for oil/water separation and simultaneous absorption of dyes and heavy metal, *Sep. Purifi. Technol.*, 2024, 333, 125904.
2. Zhu N X, Wei Z W, Chen C X, et al. Self-generation of surface roughness by low-surface-energy alkyl chains for highly stable superhydrophobic/superoleophilic MOFs with multiple functionalities. *Angew. Chem. Int. Edit.*, 2019, 58(47): 17033-40.
3. Zhang N, Qi Y F, Zhang Y N, et al. A review on the oil/water mixture separation material. *Ind. Eng. Chem. Res.*, 2020, 59(33): 14546-68.
4. Pal S, Mondal S, Pal P, et al. Fabrication of durable, fluorine-free superhydrophobic cotton fabric for efficient self-cleaning and heavy/light oil-water separation. *Colloid. Interface. Sci. Com.*, 2021, 44: 100469-481.
5. Saini H, Otyepková E, Schneemann A, et al. Hierarchical porous metal-organic framework materials for efficient oil-water separation. *J. Mater. Chem. A*, 2022, 10(6): 2751-85.
6. Wang Z, Yang X, Guan M, Li H, Guo J, Shi H, Li S, Triple-defense design of multifunctional superhydrophilic surface with outstanding underwater superoleophobicity, anti-oil-fouling properties, and high transparency, *J. Membr. Sci.*, 2024, 689, 122161.
7. Li H, Zhang J Q, Zhu L, et al. Reusable membrane with multifunctional skin layer for effective removal of insoluble emulsified oils and soluble dyes. *J. Hazard. Mater.*, 2021, 415: 125677-86.
8. Wang Z, Shao Y, Wang T, Zhang J, Cui Z, Guo J, Li S, Chen Y, Janus membranes with asymmetric superwettability for high-performance and long-term on-demand oil/water emulsion separation, *ACS Appl. Mater. Interfaces*, 2024, 16, 15558-15568.
9. Deng Y, Peng C, Dai M, et al. Recent development of super-wettable materials and their applications in oil-water separation. *J. Clean. Prod.*, 2020, 266: 121624.
10. Liu Y, Lin Z, Luo Y, et al. Superhydrophobic MOF based materials and their applications for oil-water separation. *J. Clean. Prod.*, 2023, 420: 138347.
11. Narayan Thorat B, Kumar Sonwani R. Current technologies and future perspectives for the treatment of complex petroleum refinery wastewater: A review. *Bioresour. Technol.*, 2022, 355: 127263.
12. Li H, Luo Y D, Yu F Y, et al. In-situ construction of MOFs-based superhydrophobic/superoleophilic coating on filter paper with self-cleaning and antibacterial activity for efficient oil/water separation. *Colloids. Surf. A: Physicochem. Eng. Aspects*, 2021, 625: 126976.
13. Du J C, Zhou C L, Yang Z J, et al. Conversion of solid  $\text{Cu}_2(\text{OH})_2\text{CO}_3$  into HKUST-1 metal-organic frameworks: Toward an under-liquid superamphiphobic surface. *Surf. Coat. Technol.*, 2019, 363: 282-90.
14. Zhang X, Zhao Y, Mu S, et al. Uio-66-coated mesh membrane with underwater superoleophobicity for high-efficiency oil-water separation. *ACS Appl. Mater. Interfaces*, 2018, 10(20): 17301-8.
15. Qiu L, Sun Y, Guo Z. Designing novel superwetting surfaces for high-efficiency oil-water separation: Design principles, opportunities, trends and challenges. *J. Mater. Chem. A*, 2020, 8(33): 16831-53.
16. Zarghami S, Mohammadi T, Sadrzadeh M, et al. Superhydrophilic and underwater superoleophobic membranes - a review of synthesis methods. *Prog. Poly. Sci.*, 2019, 98: 101166-205.
17. Dong X X, Cui M, Huang R L, et al. Polydopamine-assisted surface coating of mil-53 and dodecanethiol on a melamine sponge for oil-water separation. *Langmuir*, 2020, 36(5): 1212-20.
18. Tamsilian Y, Ansari-Asl Z, Maghsoudian A, et al. Superhydrophobic ZIF8/PDMS-coated polyurethane nanocomposite sponge: Synthesis, characterization and evaluation of organic pollutants continuous separation. *J. Taiwan Insti. Chem. Eng.*, 2021, 125: 204-14.
19. Zhang Y N, Zhang N, Zhou S, et al. Facile preparation of ZIF-67 coated melamine sponge for efficient oil/water separation. *Indust. Eng. Chem. Res.*, 2019, 58(37): 17380-8.
20. Zhang Y Q, Hou S Y, Song H L, et al. A green and facile one-step hydration method based on ZIF-8-pda to prepare melamine composite sponges with excellent hydrophobicity for oil-water separation. *J. Hazard. Mater.*, 2023, 451: 131064-83.
21. Chen X X, Zhang Y P, Du H L, et al. "Two birds with one stone" strategy for oil/water separation based on ni foams assembled using metal-organic frameworks. *New J. Chem.*, 2023.
22. Xiang W, Guo Z. Nonflammable, robust and recyclable hydrophobic zeolitic imidazolate frameworks/sponge with high oil absorption capacity for efficient oil/water separation. *Colloids Surf. A: Physicochem Eng Aspects*, 2022, 650: 129570.
23. Liu Y Y, Wang X, Feng S Y. Nonflammable and magnetic sponge decorated with polydimethylsiloxane brush for multitasking and highly efficient oil-water separation. *Adv. Funct. Mater.*, 2019, 29(29): 1902488-500.

24. Li X F, Yan B Y, Huang W Q, et al. Room-temperature synthesis of hydrophobic/oleophilic ZIF-90-CF3/melamine foam composite for the efficient removal of organic compounds from wastewater. *Chem. Eng. J.*, 2022, 428: 132501-14.
25. Cao M J, Feng Y, Chen Q, et al. Flexible Co-ZIF-L@melamine sponge with underwater superoleophobicity for water/oil separation. *Mater. Chem. Phys.*, 2020, 241: 122385-90.
26. Wang R X, Zhao X T, Jia N, et al. Superwetting oil/water separation membrane constructed from in situ assembled metal-phenolic networks and metal-organic frameworks. *ACS Appl. Mater. Interfaces*, 2020, 12(8): 10000-8.
27. Cai Y H, Chen D Y, Li N J, et al. Nanofibrous metal-organic framework composite membrane for selective efficient oil/water emulsion separation. *J. Membr. Sci.*, 2017, 543: 10-7.
28. Huang A S, Bux H, Steinbach F, et al. Molecular-sieve membrane with hydrogen permselectivity: ZIF-22 in ita topology prepared with 3-aminopropyltriethoxysilane as covalent linker. *Angew. Chem. Internat. Edit.*, 2010, 49(29): 4958-61.
29. Wang J Q, Xu J K, Chen G J, et al. Reversible wettability between underwater superoleophobicity and superhydrophobicity of stainless steel mesh for efficient oil-water separation. *ACS Omega*, 2020, 6(1): 77-84.
30. Li Q Q, Deng W J, Li C H, et al. High-flux oil/water separation with interfacial capillary effect in switchable superwetting Cu(OH)<sub>2</sub>@ZIF-8 nanowire membranes. *ACS. Appl. Mater. Interfaces*, 2018, 10(46): 40265-73.
31. Yang B H, Shi M B, Huang R L, et al. One-pot synthesis of fluorine functionalized Zr-MOFs and their in situ growth on sponge for oil absorption. *Colloids Surf. A: Physicochem Eng Aspects*, 2021, 616: 126322-32.
32. Azam T, Pervaiz E, Farrukh S, et al. Biomimetic highly hydrophobic stearic acid functionalized MOF sponge for efficient oil/water separation. *Mater. Res. Exp.*, 2021, 8(1): 015019-34.
33. Azam T, Pervaiz E, Javed S, et al. Tuning the hydrophobicity of MOF sponge for efficient oil/water separation. *Chem. Phys. Imp.*, 2020, 1: 100001-10.
34. Chen X Y, Wang L, Shinsuke Nagamine, et al. Study oil/water separation property of pe foam and its improvement by in situ synthesis of zeolitic-imidazolate framework (ZIF-8). *Polym. Eng. Sci.*, 2019, 59(7): 1354-61.
35. Zhang L R, Xie J L, Luo X, et al. Enhanced hydrophobicity of shell-ligand-exchanged ZIF-8/melamine foam for excellent oil-water separation. *Chem. Eng. Sci.*, 2023, 273: 118663.
36. Chen X Y, Wang L, Nagamine S, et al. Study oil/water separation property of pe foam and its improvement by in situ synthesis of zeolitic-imidazolate framework (ZIF-8). *Polym. Eng. Sci.*, 2019, 59(7): 1354-61.

**Disclaimer/Publisher's Note:** The statements, opinions and data contained in all publications are solely those of the individual author(s) and contributor(s) and not of MDPI and/or the editor(s). MDPI and/or the editor(s) disclaim responsibility for any injury to people or property resulting from any ideas, methods, instructions or products referred to in the content.